DOI: http://dx.doi.org/10.32571/ijct.1194356 **E-ISSN: 2602-277X**

International Journal of Chemistry and Technology

http://dergipark.org.tr/ijct

Research Article

Antifungal activity and optimization procedure of microwave-synthesized silver nanoparticles using linden (*Tilia rubra* subsp. *caucasica*) flower extract

Uğur YİĞİT[1] Muharrem TÜRKKAN[1 *]

[1]*Department of Plant Protection, Faculty of Agriculture, Ordu University, Ordu 52200, Türkiye*

Received: 25 October 2022; Revised: 28 November 2022; Accepted: 2 December 2022

*****Corresponding author e-mail: muharremturkkan@gmail.com

Citation: Yiğit, U.; Türkkan, M. *Int. J. Chem. Technol.* **2023**, 7(1), 25-37

ABSTRACT

The present study used linden [*Tilia rubra* DC. subsp. *caucasica* (Rupr.)] flower extract as a reducing and coating agent to create silver nanoparticles (AgNPs). The Face-Centered Central Composite Design (FCCD) of Response Surface Methodology (RSM) was used to investigate the combined effect of four different synthesis variables in order to obtain the maximum amount of AgNPs produced. Optimal AgNP production was achieved within the investigated range when the $AgNO_3$ concentration, plant extract amount, microwave power, and time were 10 mM, 2.5 ml, 800 watts, and 90 seconds, respectively. The Ultraviolet–Visible Spectroscopy (UV–Vis), Fourier Transform Infrared Spectroscopy (FT–IR), Scanning Electron Microscopy (SEM)–Energy Dispersive X-ray Spectroscopy (EDS), and Transmission Electron Microscopy (TEM) were utilized to characterize the synthesized AgNPs. In addition, *in vitro* experiments revealed that the EC_{50}, minimum inhibitory concentration (MIC), and minimum fungicidal concentration (MFC) values of synthesized AgNPs for seven *Phytophthora* (*P. cactorum*, *P. capsici*, *P. cinnamomi*, *P. citrophthora*, *P. megasperma*, *P. nicotianae*, and *P. palmivora*) species varied between 46.38 and 119.36 µg ml^{-1}, 225 and 450 µg ml^{-1}, and 225 and 900 µg ml^{-1}, respectively. The findings of this study suggest that AgNPs synthesized with linden flower extract should be investigated further for use in the treatment of *Phytophthora* spp.-caused diseases.

Keywords: Silver nanoparticles, *Tilia rubra* subsp. *caucasica*, face-centered central composite design, *Phytophthora* spp., toxicity

Ihlamur (*Tilia rubra* subsp. *caucasica*) çiçek ekstraktı kullanılarak mikrodalga aracılığıyla sentezlenen gümüş nanopartiküllerin antifungal aktivitesi ve optimizasyon prosedürü

ÖZ

Mevcut çalışmada gümüş nanopartiküller (AgNP'ler) oluşturmak için indirgeyici ve kaplayıcı etken olarak ıhlamur [*Tilia rubra* DC. subsp. *caucasica* (Rupr.)] çiçek ekstraktı kullanılmıştır. Üretilen AgNP'lerin maksimum miktarını elde etmek için dört farklı sentez değişkeninin birleşik etkisini araştırmak için Yanıt Yüzey Metodolojisi (RSM)'nin Yüz Merkezli Merkezi Kompozit Tasarım (FCCD)'ı kullanılmıştır. Optimum AgNP üretimi, $AgNO_3$ konsantrasyonu, bitki ekstrakt miktarı, mikrodalga gücü ve sürenin sırasıyla 10 mM, 2.5 ml, 800 watt ve 90 saniye olduğunda incelenen aralıkta elde edilmiştir. Sentezlenen AgNP'leri karakterize etmek için Ultraviyole Görünür Bölge Spektroskopisi (UV–Vis), Fourier Dönüşümü Kızılötesi Spektroskopisi (FT–IR), Taramalı Elektron Mikroskobu (SEM)–Enerji Dağıtıcı X-ışını Spektroskopisi (EDS) ve Geçirgen Elektron Mikroskobu (TEM) kullanılmıştır. Ayrıca *in vitro* deneyler, yedi *Phytophthora* (*P. cactorum*, *P. capsici*, *P. cinnamomi*, *P. citrophthora*, *P. megasperma*, *P. nicotianae*, and *P. palmivora*) türü için sentezlenen AgNP'lerin EC_{50}, minimum engelleyici konsantrasyon (MIC) ve minimum fungisidal konsantrasyon (MFC) değerlerinin sırasıyla 46.38 ve 119.36 µg ml^{-1}, 225 ve 450 µg ml^{-1}, ve 225 ve 900 µg ml^{-1} arasında değiştiğini ortaya koymuştur. Bu çalışmanın bulguları, ıhlamur çiçek ekstraktı ile sentezlenen AgNP'lerin, *Phytophthora* türlerinin neden olduğu hastalıkların mücadelesinde kullanılmak üzere daha fazla araştırılması gerektiğini önermektedir.

Anahtar Kelimeler: Gümüş nanopartiküller, *Tilia rubra* subsp. *caucasica*, yüz merkezli merkezi kompozit tasarım, *Phytophthora* spp., zehirlilik

This research was produced from the doctoral thesis of the first author.

DOI: http://dx.doi.org/10.32571/ijct.1194356 E-ISSN: 2602-277X

1. INTRODUCTION

Nanomaterials have unique physical and chemical properties that cannot be observed in bulk or molecular form.[1] Silver nanoparticles (AgNPs) in particular are gaining popularity due to their optical, catalytic, mechanical, electrical, and biosensing properties.[2-4] AgNPs have strong antimicrobial activity and are used as a component of human health drugs in the pharmaceutical industry.[5] Numerous studies have shown that AgNPs can be produced using physical and chemical methods, but due to the use of toxic chemicals in the synthesis process, an alternative method must be found.[6-12] In this regard, the biological approach, which is based on living organisms such as bacteria, fungi, lichens, and plants, provides a reliable, simple, quick, non-toxic, and environmentally friendly solution.[13-16] Plants are the most popular bio-resource because they are easily accessible, non-toxic, and easy to process. Plants also contain a large number of biologically active compounds, such as polyphenols, organic acids, and proteins, which act not only as reducing agents but also as stabilizing agents, making synthesis simple.[17-18] Gardea-Torresdey was the first to report on the green synthesis of nano-sized AgNPs using alfalfa sprouts (variety Mesa).[19] AgNPs have recently been reported to synthesize with leaf extracts of *Acalypha indica*[20], *Camellia japonica*[21], *Nigella arvensis*[22], *Malva parviflora*[23], and *Psidium guajava*[24]; flower extract of *Clitoria ternatea*[25]; fruit extracts of *Rubus glaucus*[26], and *Diospyros malabarica*[27]; bark extracts of *Cinnamon zeylanicum*[28], *Alstonia scholaris*[29], and *Prosopis juliflora*[30]; peel extract of *Musa paradisiaca*[31]; root extract of *Berberis vulgaris*[32]; rhizome extract of *Zingiber officinale*[33]; tuber extract of *Pueraria tuberosa*[34]; and seed extracts of *Jatropha curcas*[35] and *Macrotyloma uniflorum*[36]. Some of the AgNPs synthesized with these plant extracts had antibacterial and/or antifungal activity. For instance, Al-Otibi and co-workers[23] determined that AgNPs synthesized from *Malva parviflora* had a strong fungistatic effect on the mycelial growth of *Alternaria alternata*, *Helminthosporium rostratum*, *Fusarium solani*, and *F. oxysporum*. *Acalypha indica*-derived AgNPs, on the other hand, were found to be highly effective against some sclerotial fungi.[20]

Tilia is a genus of 25 species in the Tiliaceae family that is distributed in East Asia, Europe-West Siberia, and North America.[37] *Tilia rubra* DC. subsp. *caucasica* (Rupr.) is the dominant linden species in the flora extending from the Black Sea Region's eastern part (Melet river) to the Caucasus Mountains' southern slopes.[38] Linden flowers are used in Turkish traditional medicine to treat indigestion, headaches, cold flu, insomnia, high blood pressure, cholesterol, and atherosclerosis[39], as well as their diaphoretic, antispasmodic, and expectorant properties.[40] On the other hand, it has been documented that linden flowers have limited antifungal[41] and antibacterial[42] activity. Linden flowers contain various biologically active compounds such as flavonoids, mucilage, essential oil, phenolic acids, amino acids, and proanthocyanidins[43,40], which serve to produce AgNPs by mediating the reduction of Ag ions.[44]

A statistical and graphical technique, Response Surface Methodology (RSM), is a widely used methodology for designing models and analyzing various manufacturing issues.[45] RSM assists in identifying factors, investigating interactions, determining optimal conditions, computing the optimal level of variables, and ensuring maximum output in a fixed number of experiments.
The study aims to optimize the production of microwave-synthesized AgNPs using *T. rubra* subsp. *caucasica* extracts with RSM based on the face-centered central composite design (FCCD), characterize the synthesized nanoparticles by various spectroscopic and microscopic methods, and evaluate their antifungal effects on some *Phytophthora* species.

2. MATERIALS AND METHODS

2.1. Plant material, chemicals, and fungal cultures

Tilia rubra subsp. *caucasica* flowers were collected from Gülyalı county, Ordu province, Türkiye. Merck (Darmstadt, Germany) supplied the silver nitrate ($AgNO_3$), sodium hydroxide (NaOH), and agar agar medium.

Phytophthora (*P. cactorum*, *P. capsici*, *P. cinnamomi*, *P. citrophthora*, *P. megasperma*, *P. nicotianae*, and *P. palmivora*) isolates used in this study were provided by Dr. Ilker Kurbetli at Batı Akdeniz Agricultural Research Institute (BATEM).

2.2. Preparation of linden flower extract

Linden flowers were washed with distilled water and dried in an oven at 60 °C after being dehumidified with paper towels. Ten grams of the flowers were mixed with 100 ml of distilled water in a 500-ml flask and stirred continuously for 30 min at 80 °C using a heater stirrer. After cooling, the extracts were centrifuged and filtered through Whatman No. 1 filter paper and then kept in a refrigerator at 4 °C.

2.3. Green synthesis of AgNPs

For the green synthesis of AgNPs in this study, 2.5–7.5 ml of linden flower extract were added to 1–10 mM $AgNO_3$ solution, and the mixture (25 ml) was stirred

DOI: http://dx.doi.org/10.32571/ijct.1194356 E-ISSN: 2602-277X

using a magnetic stirrer. The final pH of the mixture was adjusted to 12 with 0.1 M NaOH. The mixture was heated in a microwave for 30 to 90 seconds at a power range of 400 to 800 watts. Silver ion reduction resulted in a color change from yellowish to brownish or dark brown depending on the reaction conditions. The synthesized AgNPs were centrifuged at 15000 rpm for 15 minutes, then washed twice with distilled water and dried at 80 °C. They were then stored in the refrigerator at 4 °C.

2.4. Statistical optimization of AgNPs synthesis

The face-centered central composite design (FCCD) from RSM was used to evaluate the effect of independent variables [$AgNO_3$ concentration (mM), linden flower extract (ml), power (watt), and time (sec.)] on AgNP synthesis and to identify an optimum condition. Each variable was coded at three levels of +1 (high), 0 (middle) and, -1 (low) (Table 1). An FCCD was designed, consisting of a total of 29 runs with five repetitions at the central point (Table 2). Response variables were fitted into the quadratic polynomial model, which is normally defined as a relationship between responses and independent variables: where Y is the absorbance of AgNPs (response), β_0 is the regression coefficient, β_i, β_{ii}, and β_{ij} are the linear, quadratic and interaction coefficients, X_i and X_j are the independent variables (factors), and ε is the error.

$$y = \beta_0 + \sum_{i=1}^{k} \beta_i X_i + \sum_{i=1}^{k} \beta_{ii} X_i^2 + \sum_{i=1}^{k-1} \sum_{j=1}^{k} \beta_{ij} X_i X_j + \varepsilon$$

Table 1. Level of variables chosen for the face-centered central composite design

Coded	Variables	Units	Min.	Max.	Coded		Mean	Std. Dev.
					Low	High		
A	$AgNO_3$ concentration	mM	1.0	10.0	1 ↔ 1.0	1 ↔ 10.0	5.5	3.61
B	Extract	ml	2.5	7.5	1 ↔ 2.5	1 ↔ 7.5	5.0	2.00
C	Power	watt	400.0	800.0	1 ↔ 400.0	1 ↔ 800.0	600.0	160.36
D	Time	sec	30.0	90.0	1 ↔ 30.0	1 ↔ 90.0	60.0	24.05

Table 2. Face-centered central composite design showing actual values along with the experimental and predicted responses

Std. order*	Run order	A-$AgNO_3$ concn. (mM)	B-Extract (ml)	C-Power (watt)	D-Time (sec)	Actual (Absorbance)	Square root transform	
							Actual	Predicted
8	1	10	7.5	800	30	0.2179	0.466798	0.472825
15	2	1	7.5	800	90	0.1257	0.354542	0.371875
21	3	5.5	5	400	60	0.1511	0.388716	0.400669
4	4	10	7.5	400	30	0.1852	0.430349	0.413638
18	5	10	5	600	60	0.3478	0.589746	0.593934
12	6	10	7.5	400	90	0.3198	0.565509	0.577405
6	7	10	2.5	800	30	0.2760	0.525357	0.569602
2	8	10	2.5	400	30	0.2840	0.532917	0.507788
1	9	1	2.5	400	30	0.0306	0.174929	0.208229
20	10	5.5	7.5	600	60	0.1483	0.385097	0.424879
25	11	5.5	5	600	60	0.1802	0.424500	0.440307
19	12	5.5	2.5	600	60	0.2372	0.487032	0.442635
28	13	5.5	5	600	60	0.2088	0.456946	0.440307
26	14	5.5	5	600	60	0.2018	0.449222	0.440307
10	15	10	2.5	400	90	0.3828	0.618708	0.639426
3	16	1	7.5	400	30	0.0503	0.224277	0.237366
16	17	10	7.5	800	90	0.6396	0.799750	0.775398
24	18	5.5	5	600	90	0.2507	0.500700	0.519448
9	19	1	2.5	400	90	0.0431	0.207605	0.193783
11	20	1	7.5	400	90	0.0843	0.290345	0.255049
5	21	1	2.5	800	30	0.0435	0.208567	0.188876
29	22	5.5	5	600	60	0.1761	0.419643	0.440307
22	23	5.5	5	800	60	0.2566	0.506557	0.489989
27	24	5.5	5	600	60	0.1913	0.437379	0.440307
7	25	1	7.5	800	30	0.0516	0.227156	0.215387
17	26	1	5	600	60	0.0631	0.251197	0.242393
13	27	1	2.5	800	90	0.0827	0.287576	0.313235
23	28	5.5	5	600	30	0.1590	0.398748	0.375385
14	29	10	2.5	800	90	0.7412	0.860930	0.840045

*Standard order

DOI: http://dx.doi.org/10.32571/ijct.1194356 E-ISSN: 2602-277X

All analyses were performed with version 13 of the Design Expert program (Stat-Ease, Inc., USA). The program was used for regression analysis of the obtained data and to estimate the regression equation coefficient. The fitted model was then plotted in the form of perturbation, 3D, and 2D contour plots to illustrate the relationship between responses. Finally, to validate the developed model, experimental sets were created using the suggested optimum combination.

2.5. Characterization of AgNPs

Preliminary characterization of the synthesized AgNPs was performed using UV–Vis Spectroscopy (Lambda 35, Perkin Elmer, Inc., MA, USA). A 200 µl solution containing AgNPs was diluted with 2 ml of distilled water. The spectra of AgNPs were obtained in the wavelength range of 200–700 nm at 1 nm resolution using a quartz cuvette. Baseline correction was done using distilled water as the blank.

Infrared spectra of the AgNPs were recorded using Fourier Transform Infrared (FT–IR) Spectroscopy (Spectrum 65, Perkin Elmer, Inc., MA, USA). 1 mg of the synthesized AgNPs was mixed with 200 mg KBr, then pressed into a pellet. The FT–IR spectra from the nanoparticles were collected in the transmittance mode at a wave number range of 4000-400 cm^{-1}.
Elemental and morphological analysis of the AgNPs were carried out with a Scanning Electron Microscope (SEM) (SU-1510, Hitachi High-Tech., Tokyo, Japan) coupled with Energy Dispersive X-ray Spectroscopy (EDS).

A Transmission Electron Microscope (TEM) (HighTech HT7700, Hitachi High-Tech., Tokyo, Japan) was used to confirm the particle size and structure of the AgNPs.

2.6. Antifungal effect of the synthesized AgNPs on *Phytophthora* species

Antifungal activities of the synthesized AgNPs on seven *Phytophthora* (*P. cactorum*, *P. capsici*, *P. cinnamomi*, *P. citrophthora*, *P. megasperma*, *P. nicotianae*, and *P. palmivora*) species were tested according to Türkkan[46] with a small modification. Different concentrations of AgNPs (28.125, 56.25, 112.5, 225, 450, and 900 µg ml^{-1}) were added to autoclaved and then cooled V8 agar medium at 50 °C. A 15-ml aliquot of modified V8 medium was aseptically dispensed into a Petri plate (7 cm in diameter) with an unmodified V8 agar plate used as a control. A 5 mm-diameter mycelial disc from 7-day-old fungal cultures was placed in the center of each plate and incubated at 25 °C in the dark after sealing the plates with Parafilm. When control growth covered plates (4–7 days), all fungal growth diameters were converted to percent inhibition compared to controls.

A probit analysis of the SPSS (Version 22; IBM Company, Chicago, USA) was used to compute the concentrations of the AgNPs that caused a 50% reduction (EC_{50}) in the fungal growth. The minimum inhibitory concentration (MIC) value, which completely stopped the fungal growth, was also found by parallel experiments.

The toxicity (fungistatic/fungicidal) of the AgNPs was evaluated according to Thompson[47] and Tripathi and co-workers[48]. V8 agar discs from modified plates that exhibited no fungal growth were re-inoculated with unmodified V8 agar plates and then monitored for 9 days at 25 °C for revivals of growth. The minimum fungicidal concentration (MFC) value was determined at the end of this period as the minimum AgNPs concentration required to completely and irreversibly stop fungal growth.

3. RESULTS AND DISCUSSION

Over the last two decades, numerous studies have demonstrated the use of various plant extracts for the green synthesis of AgNPs.[19,20,23,25,26,28,29,31-35] In this study, linden flower extract was used as a reducing and stabilizing agent in the green synthesis of AgNPs.

3.1. Optimization of process parameters by response surface methodology

In the study, we used the face-centered central composite design (FCCD) to determine the optimum experimental condition for the synthesis of AgNPs from linden flowers. Considering the peak intensity, four independent synthesis factors, including the concentration of $AgNO_3$ solution, linden flower extract (ml), power (watt), and time (sec.), were investigated to obtain the optimal SPR band of the synthesized AgNPs.

Previous studies have shown that pH is one of the most effective factors in the synthesis of AgNPs. For instance, Veerasamy and co-workers[49] reported that high pH values facilitate the binding of more AgNPs with many functional groups available for silver bonding. According to Vanaja and co-workers[50], the formation of nanoparticles increased with increasing pH. Khalil and co-workers[51] demonstrated that synthesis of AgNPs using olive leaf extract under alkaline conditions improved the antioxidants' reducing and stabilizing ability. As a result, the pH values of alkaline solutions (8, 10, and 12) were used in the current study (Figure 1). The FCCD for the four factors with a solution pH of 12 was constituted with a total of 29 runs. The SPR peak intensity of AgNPs was determined using responses resulting from the absorbance of 29 runs synthesized in the 372-401 nm range (Table 2).

DOI: http://dx.doi.org/10.32571/ijct.1194356 E-ISSN: 2602-277X

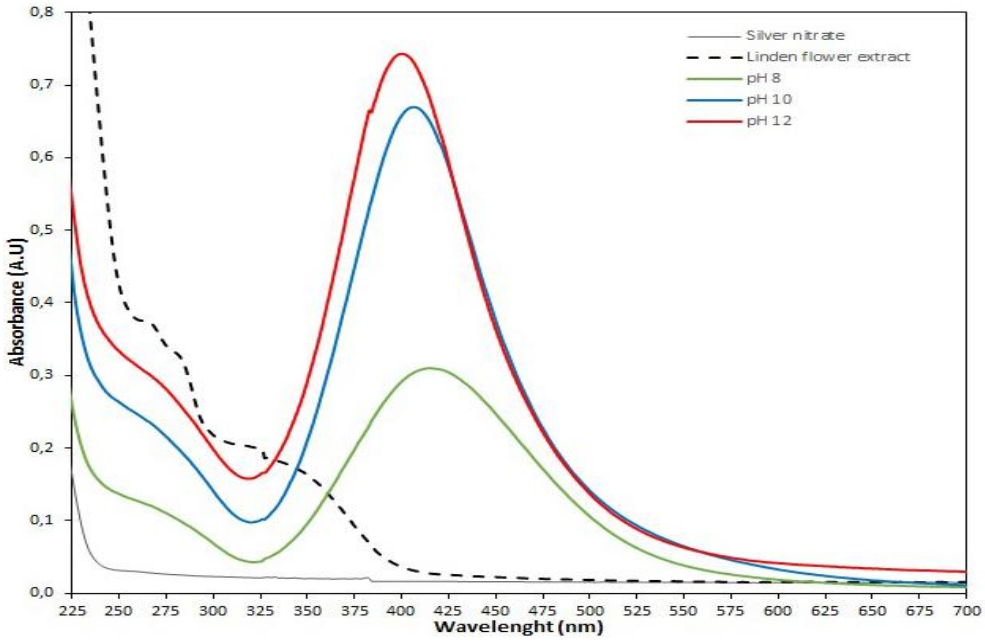

Figure 1. UV–Vis spectra of AgNPs synthesized with linden flower extract under alkaline conditions.

The model expressing the relationship between experimental factors and response to determine optimal values of AgNP synthesis is presented in Eq. (1) and Eq. (2):

$$Y(coded)=0.4403+0.1758A-0.0089B+0.0447C+0.0720D-0.0221A^2-0.0065B^2+0.0050C^2+0.0071D^2-0.0308AB+0.0203AC+0.0365AD-0.0007BC+0.0080BD+0.0347CD \quad (1)$$

$$Y(actual)=+0.304280+0.035028A+0.016359B-0.000392C-0.004040D-0.001093A^2-0.001048B^2+0.000000125551C^2+0.00000789931D^2-0.002740AB+0.000023AC+0.000271AD-0.0000013291BC+0.000107BD+0.00000578358CD \quad (2)$$

Where Y is the obtained absorbance (square root transformation, sqrt) as an indication of the SPR intensity; A is silver nitrate concentration; B is the linden flower extract; C is the power and D is the time. In the present study, data transformation is required since the ratio of maximum (0.7412) to minimum (0.0306) among responses is greater than 10. Therefore, before statistical analysis, the response was transformed to fit a normal distribution using sqrt. The significance of this quadratic model was assessed using analysis of variance (ANOVA) (Table 3).

Table 3. ANOVA for absorption response

Source	Sum of Squares	df	Mean Square	F-value	p-value	
Model	0.7528	14	0.0538	51.17	< 0.0001	significant
A-$AgNO_3$ concentration (mM)	0.5561	1	0.5561	529.2	< 0.0001	
B-Extract (ml)	0.0014	1	0.0014	1.35	0.2647	
C-Power (watt)	0.0359	1	0.0359	34.16	< 0.0001	
D-Time (sec.)	0.0934	1	0.0934	88.87	< 0.0001	
AB	0.0152	1	0.0152	14.46	0.0019	
AC	0.0066	1	0.0066	6.27	0.0253	
AD	0.0213	1	0.0213	20.31	0.0005	
BC	6.90E-06	1	6.90E-06	0.0066	0.9366	
BD	0.001	1	0.001	0.9823	0.3385	
CD	0.0193	1	0.0193	18.33	0.0008	
A^2	0.0013	1	0.0013	1.21	0.2906	
B^2	0.0001	1	0.0001	0.1056	0.7501	
C^2	0.0001	1	0.0001	0.0621	0.8069	
D^2	0.0001	1	0.0001	0.1244	0.7296	
Residual	0.0147	14	0.0011			
Lack of Fit	0.0137	10	0.0014	5.46	0.058	not significant
Pure Error	0.001	4	0.0003			
Cor Total	0.7675	28				

DOI: http://dx.doi.org/10.32571/ijct.1194356 E-ISSN: 2602-277X

The model F-value of 51.17 implies that the model is statistically significant. There is only a 0.01% chance that an F-value this large could occur due to noise, while p-values are 0.0001. P-values less than 0.05 indicate that the developed quadratic model and some terms are significant. A lack of fit of 5.46 (F-value) compared to pure error means it is negligible and is a good indicator for the model. In our study, the regression value (R^2 = 0.9808) means that 98.08% of both observed and predicted data can be explained by using this model (Figure 2a, Table 4). Moreover, the predicted R^2 of 0.8760 is in reasonable agreement with the adjusted R^2 of 0.9617, since the difference between the two is less than 0.2. It is reported that a suitable statistical model should result in R^2~1.[52] Adequate precision measures the signal-to-noise ratio, and a ratio greater than 4 is desirable. The ratio of 27.93 indicated an adequate signal; hence, this model can be used to continue the design process. In the developed model, the residuals show a random distribution between the predicted and actual (observed) values, which indicates that all the residual values lie along a straight line without large deviations, confirming the normality of the error distribution (Figure 2b). It is also shown in Figure 2(c) that not only is the residue randomly distributed on both sides of the zero line, but it is also within the acceptable range. Mondal and Purkait[53] stated that the residuals between predicted and actual values should be in the range of ±3%, demonstrating that the constructed model is adequate. The perturbation plot shows that $AgNO_3$ concentration (A) has a greater positive effect than the other three factors in increasing the amount of silver nanoparticle synthesis (Figure 2d).

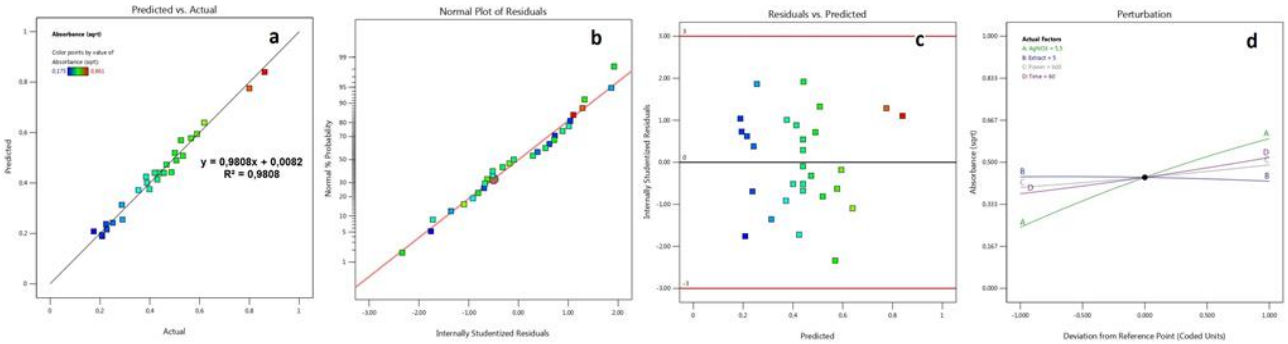

Figure 2. Diagnostic plots of AgNPs optimized using FCCD: (a) Predicted vs. Actual, (b) Normality, (c) Residual vs. Predicted, (d) Perturbation.

Table 4. Fit and model summary statistics

Std. Dev.	0.0324	R^2	0.9808
Mean	0.43	Adjusted R^2	0.9617
C.V. %	7.54	Predicted R^2	0.876
		Adeq Precision	27.9303
PRESS	0.0952	-2 Log Likelihood	-137.71
BIC	-87.20	AICc	-70.78

In the study, 3D and 2D contour plots were used to show the interactions among variables and their mutual effects on the absorbance (Figure 3). The relationship between $AgNO_3$ concentration and the extract is depicted in Figure 3(a). AgNP synthesis tends to be higher, especially under conditions where the $AgNO_3$ concentration is 10 mM and the extract is between 2.5 and 3.5. On the contrary, the production of AgNPs is maximized when it comes to the same concentration of $AgNO_3$, the highest power level, and the longest duration of time (Figure 3b, 3c). Moreover, the relationship between $AgNO_3$ concentration and power was similar to that of $AgNO_3$ concentration and time. When the extract interacts with power or time, it appears to have a limited effect on the synthesis of AgNPs, as shown in Figures 3(d) and 3(e). The synthesis of AgNPs, on the other hand, reaches its peak when both power and time are at their peak (Figure 3f). These findings are consistent with those of Cai and co-workers[54], who reported that by adjusting power and time, total energy (power x time) is optimized over a specific range of 700-850 watts min 100 ml^{-1}, resulting in high-quality output. Furthermore, they discovered that if the total energy is less than 700 watts min, Ag ions cannot be fully reduced, resulting in low AgNP synthesis. Nikaeen and co-workers[55] found that the effects of $AgNO_3$ concentration and time on SPR intensity were similar, and that higher concentrations of both increased the quality of AgNPs. For the synthesis of AgNPs, Krishnaraj and co-workers[20] revealed that 50 ml of reaction medium containing 6 ml of *A. indica* leaf extract and 1 mM of $AgNO_3$ solution is optimum.

DOI: http://dx.doi.org/10.32571/ijct.1194356 E-ISSN: 2602-277X

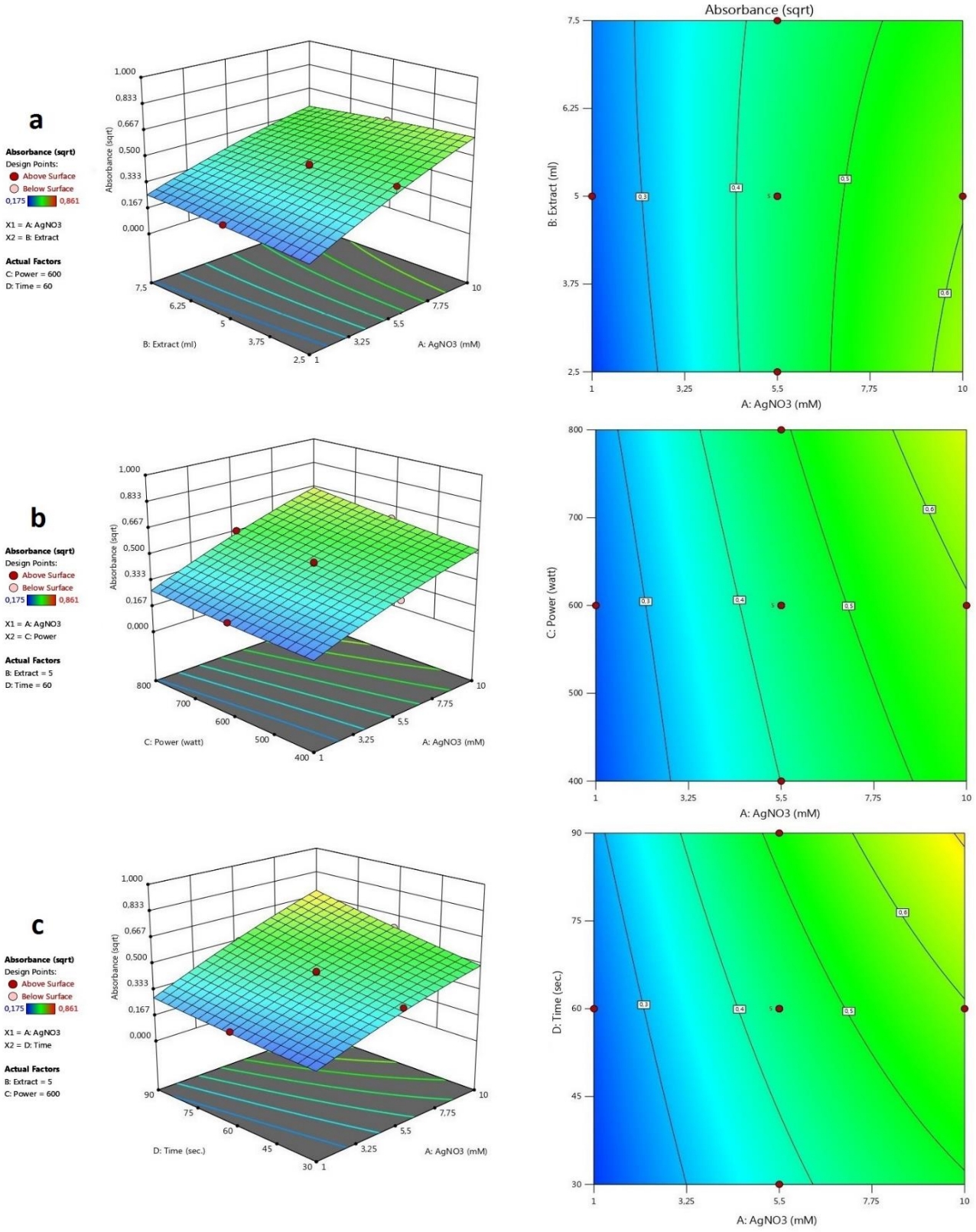

Figure 3. 3D and 2D plots showing the combined effects of factors affecting the synthesis of AgNPs: (a) $AgNO_3$ concentration and linden flower extract, (b) $AgNO_3$ concentration and power, and (c) $AgNO_3$ concentration and time.

DOI: http://dx.doi.org/10.32571/ijct.1194356 E-ISSN: 2602-277X

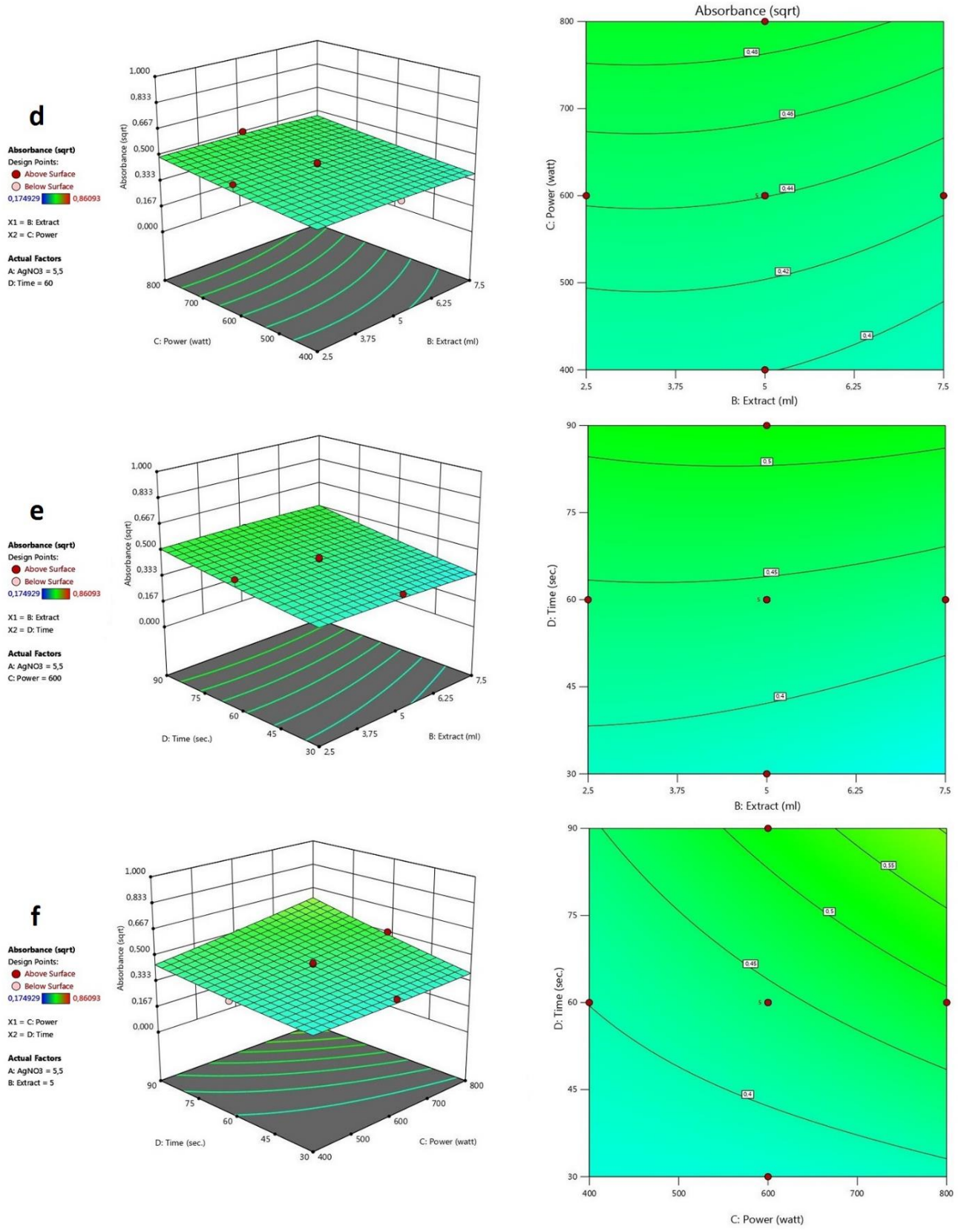

Figure 3. 3D and 2D plots showing the combined effects of factors affecting the synthesis of AgNPs: (d) linden flower extract and power, (e) linden flower extract and time, and (f) power and time.

DOI: http://dx.doi.org/10.32571/ijct.1194356 E-ISSN: 2602-277X

In our study, the optimum values of $AgNO_3$ concentration, extract volume, power, and time for the synthesis of AgNPs at 401 nm are 10mM, 2.5 ml, 800 watts, and 90 sec., respectively, and the the predicted absorbance value of the corresponding AgNPs is 0.840 (Table 5). We repeated the experimental synthesis of AgNPs using the parameters mentioned above and obtained an absorbance value of 0.896 with an error value of 3.2%, which is less than the 20% (0.2) error value. Because the error value is much lower than the standard value (0.2) of Design Expert software, it has been verified that it is sufficient for model parameter optimization.

Table 5. Validation of experimental model

Experiments	Absorbance (401 nm)	Absorbance (Sqrt)	Absorbance (Predicted)
1	0.8031	0.8962	-
2	0.7921	0.8900	-
3	0.8069	0.8983	-
4	0.7994	0.8941	-
5	0.8130	0.9017	-
Average	0.8029	0.8960	0.840

3.2. Characterization of AgNPs

3.2.1. UV–Vis spectral analysis

UV-Vis spectroscopy was used to determine the absorbance spectra of the synthesized AgNPs. AgNPs synthesized under optimum conditions caused a dark brown color change, which is a sign of reduction of silver ions in solution from Ag^{+1} to Ag^0. This is due to the excitation of the SPR of AgNPs.[56] Figure 4 shows the absorbance spectra of silver colloid as a function of the reactions of Ag ions with the linden flower extract. The characteristic absorbance peak of AgNPs in the study was observed at 401 nm (Figure 4), which is within the range previously reported for AgNPs. [57,58]

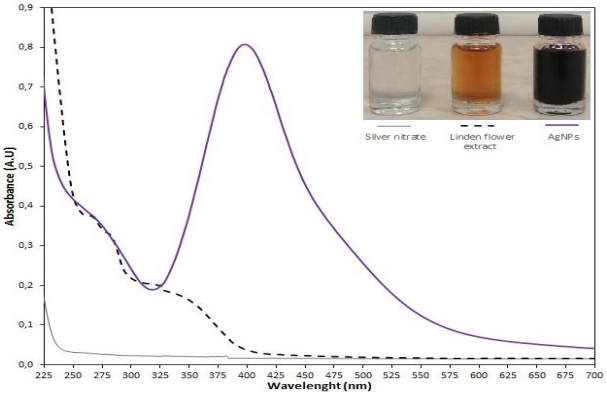

Figure 4. Visual observation and UV–Vis spectra of AgNPs synthesized with linden flower extract under optimum conditions.

3.2.2. FT–IR studies

The functional groups of both the linden flower extract and the synthesized AgNPs were determined by FT-IR analysis. FT-IR spectrum of the plant extract showed nine major peaks at 3248.13 (O–H stretching, alcoholic or phenolic), 2931.80 (C–H and CH_2; aliphatic hydrocarbons), 2322.29 (O=C=O stretching), 2129.41 (C≡C stretching, alkyne), 1589.34 (C=C), 1388.75 (C–O, ester group), 1234.44 (C–O, cyclic polyphenolics), 1049.28 (O–H deformation) and 663.51 (C–C bending) cm^{-1} (Figure 5a). Flavonoid and phenolic compounds could be adsorbed on the surface of AgNPs, possibly by the interaction through π-electrons interaction.[44] The carbonyl and hydroxyl linkages in the components of linden flower extract are responsible for the reduction of silver ions to AgNPs. On the other hand, in the FT-IR spectrum of AgNPs, different peaks were observed between 3556.74 cm and 1126.43 cm, originating from the O–H, N–H, C=C, C–N, and C–O groups (Figure 5b). It also reveals the possible interaction between Ag ions and linden flower extract during the bioreduction stage.

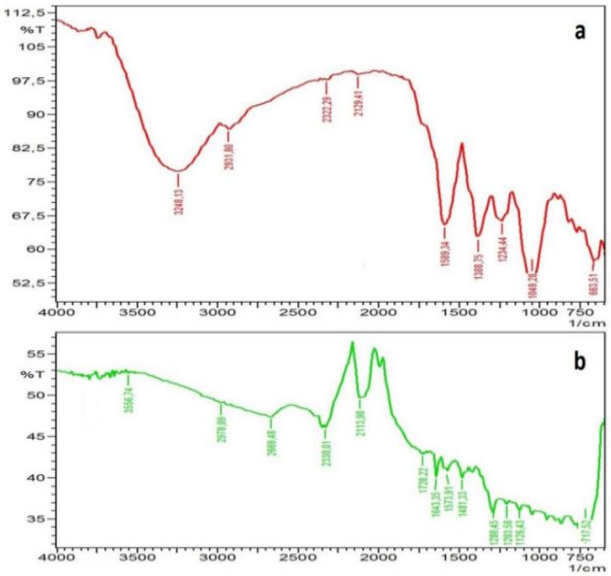

Figure 5. FT–IR spectra of (a) linden flower extract and (b) AgNPs synthesized with linden flower extract.

3.2.3. SEM–EDS and TEM analyzes

The size, shape, and morphologies of the synthesized AgNPs were characterized by SEM–EDS and TEM. SEM (Figure 6a) and TEM (Figure 6b) data revealed that the AgNPs were nearly spherical in shape and ranged in size from 9.92 to 87.34 nm, with an average particle size of 24.77 nm. Also, a few clusters were noticed in the SEM image. In EDS profiles, the AgNPs with crystalline character were determined to have a peak in the 3KeV area (Figure 6c), which is consistent with the results of previous studies. Vijayaraghavan and co-workers[59] observed an absorption spectrum at 3KeV with a strong peak at the silver region confirming the presence of AgNPs. It has also been reported that this may be due to the SPR property of AgNPs.[60] EDS spectral data revealed that the nanoparticles were composed primarily of silver, and the two prominent contaminants were phosphorus

DOI: http://dx.doi.org/10.32571/ijct.1194356 E-ISSN: 2602-277X

(P) and calcium (Ca), possibly from linden flower extract. In addition, carbon (C), and oxygen (O) were found in the residual materials surrounding the nanoparticles and the SEM grid used to prepare them. EDS mapping of the nanoparticles is shown in Figure 6(d), where Ag, C, O, and Ca are expressed as green, yellow, red, blue, and purple color, respectively.

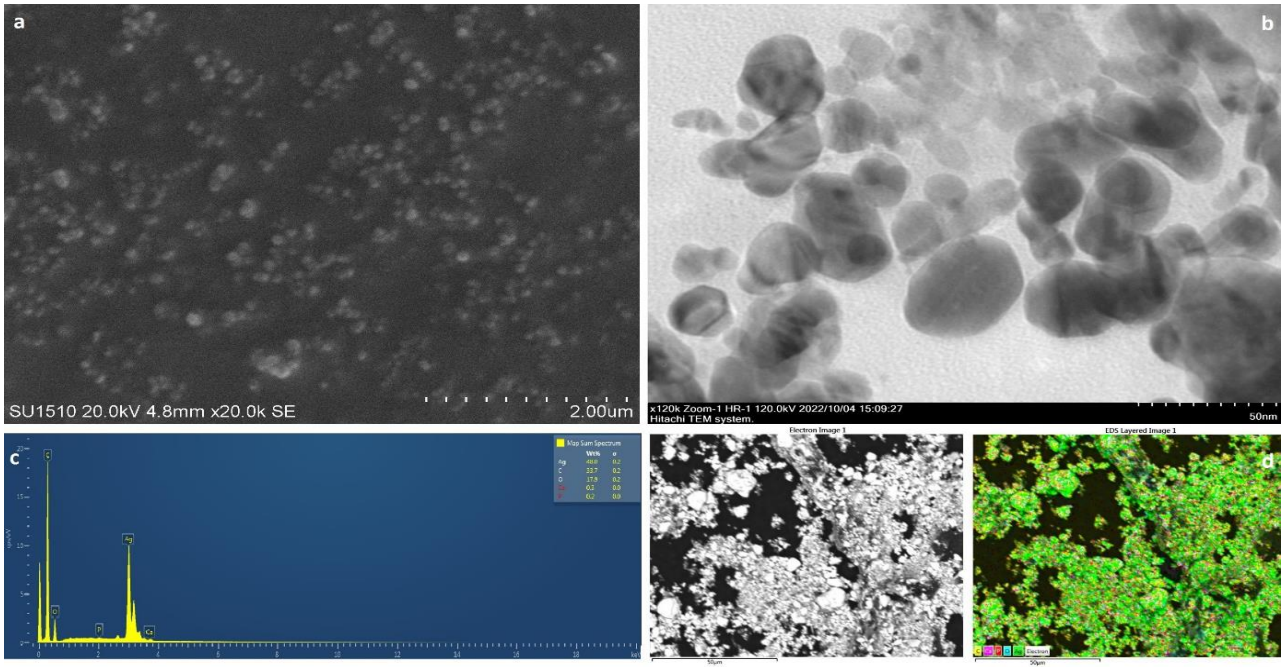

Figure 6. Microscopic and elemental analyses of synthesized AgNPs are based on (a) SEM image, (b) TEM image, (c) EDS spectrum, and (d) SEM–EDS mapping approach.

3.3. Antifungal activity of the synthesized AgNPs

Of the *Phytophthora* isolates tested in this study, *P. cactorum* and *P. palmivora* were more sensitive to the AgNPs than others (Table 6). EC_{50} values of AgNPs for *Phytophthora* isolates ranged from 46.38 to 119.36 µg ml^{-1}. At concentrations of 225 or 450 µg ml^{-1} AgNPs, mycelial growth of all 7 *Phytophthora* isolates was completely stopped (Figure 7). Furthermore, at 225 µg ml^{-1}, the inhibitory effect was fungicidal for *P. cactorum* and *P. palmivora* but fungistatic for *P. megasperma* and *P. cinnamomi*, whose inoculums began to grow when transferred to fresh V8 agar medium and then covered all Petri plates within a few days. The fungicidal effect of AgNPs was observed at 450 µg ml^{-1} for the remaining 4 *Phytophthora* species, with the exception of *P. cinnamomi*. In several previous studies, AgNPs synthesized by different plant extracts have been shown to have potent antifungal activity against various phytopathogenic fungi. Krishnaraj and co-workers[20] reported that the mycelial growth of some sclerotial fungi, including *Botrytis cinerea*, *Macrophomina phaseolina*, *Rhizoctonia solani*, and *Sclerotinia sclerotiorum*, was greatly suppressed by *Acalypha indica* AgNPs at a concentration of 1500 µg ml^{-1}. Al-Zahrani and Al-Garni[61] determined that the MIC values of AgNPs synthesized using *Allium ampeloprasum* ranged from 652 to 2500 µg ml^{-1} for different *Aspergillus* species. On the other hand, AgNPs synthesized using *Artemisia absinthium* were observed to have a much lower MIC value than 100 µg ml^{-1} against different *Phytophthora* species such as *P. capsici*, *P. cinnamomi*, *P. infestans*, *P. katsurae*, *P. palmivora*, *P. parasitica*, and *P. tropicalis*.[62] However, these differences may be due to the biochemical content of the plants that mediate the synthesis of AgNPs and the difference in target organisms. It is assumed that the toxicity of silver nanoparticles is related to their very small structure, shape, and form, and that silver nanoparticles act by disrupting the normal functions of cell organelles after penetrating the microbial cell.[63]

Table 6. Toxic effects of AgNPs synthesized with linden flower extract against some *Phytophthora* species

***Phytophthora* spp.**	**EC_{50}[a] (µg ml^{-1})**	**MIC[b] (µg ml^{-1})**	**MFC[c] (µg ml^{-1})**
P. cactorum	50.66	225	225
P. capsici	110.38	450	450
P. cinnamomi	46.38	225	900
P. citrophthora	119.36	450	450
P. megasperma	96.37	225	450
P. nicotianae	77.27	450	450
P. palmivora	91.71	225	225

[a]The concentration that caused 50% reduction.
[b]Minimum inhibitory concentration.
[c]Minimum fungicidalconcentration.

DOI: http://dx.doi.org/10.32571/ijct.1194356 E-ISSN: 2602-277X

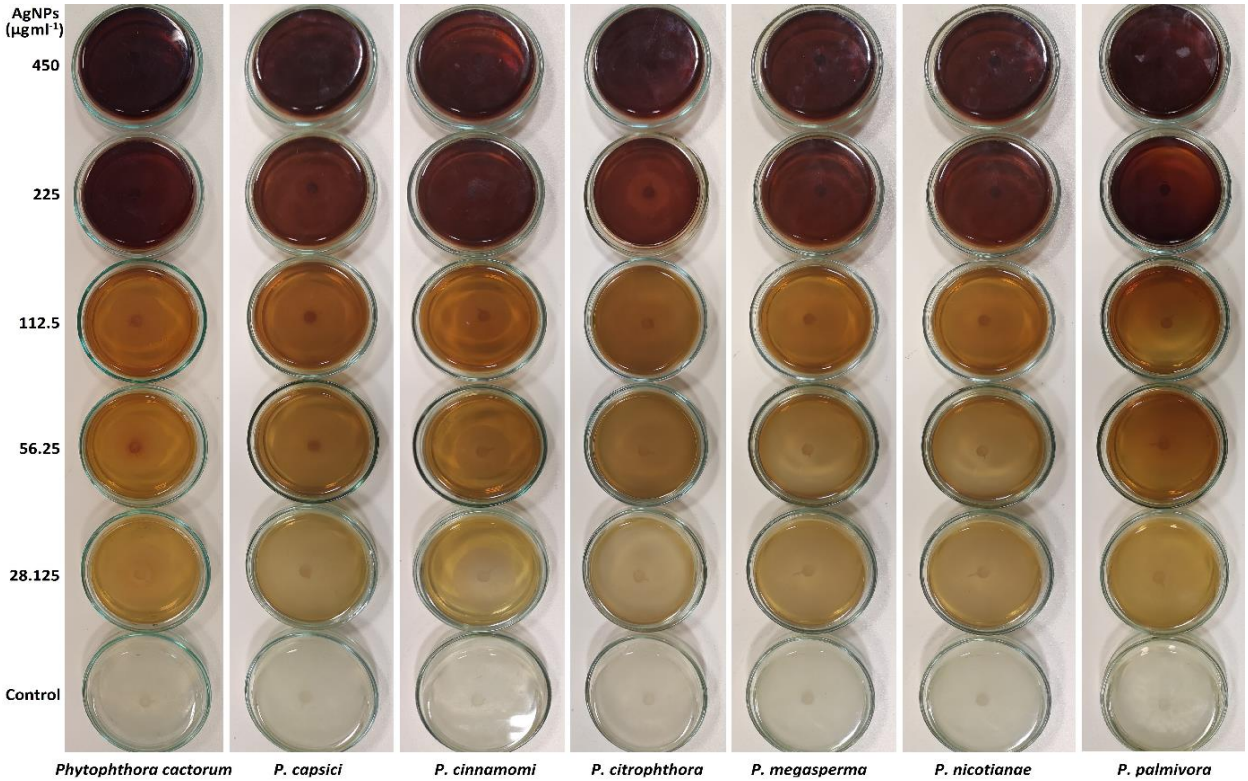

Figure 7. Effects of the different concentrations of synthesized AgNPs on *Phytophthora* species.

4. CONCLUSIONS

In this study, AgNPs were synthesized by a green method using linden (*Tilia rubra* subsp. *caucasica*) flower extract. Based on the RSM, the FCCD was used to optimize four important experimental parameters in the biosynthesis process of AgNPs, such as $AgNO_3$ concentration, extract volume, power, and time. Through a four-factor equation, the FCCD with 29 runs, the optimum conditions of the experimental parameters are computed as 10 mM, 2.5 ml, 800 watts, and 90 seconds, and this reaction condition was experimentally verified. The synthesized AgNPs were characterized by UV–Vis, FT–IR, SEM–EDS, and TEM. In addition, the synthesized AgNPs exhibited antifungal activity against some important *Phytophthora* species, such as *P. cactorum*, *P. capsici*, *P. cinnamomi*, *P. citrophthora*, *P. megasperma*, *P. nicotianae*, and *P. palmivora*.

ACKNOWLEDGEMENTS

This study, supported by Ordu University (The project no: B-2209), is part of the first author's doctoral thesis. We also thank Dr. İlker Kurbetli for providing *Phytophthora* isolates.

Conflict of interests

I declare that there is no conflict of interest with any person, institute, company, etc.

REFERENCES

1. Ahn, E.Y.; Park, Y. *Mater. Sci. Engin*. **2020**, C, 116, 111253.

2. Jain, R.K.; Huang, X.; El-Sayed, I.H.; El-Sayed, M.A. *Acc. Chem. Res.* **2008**, 41, 1578-1586.

3. Tran, Q.H.; Le, A.T. *Adv. Nat. Sci.: Nanosci. Nanotechnol. 4*. **2018.**

4. Wei, L.; Lu, J.; Xu, H.; Patel, A.; Chen, Z.S.; Chen, G. *Drug Disc. Tod*. **2015**. 20, 595.

5. Lansdown, A.B. *Advanc. Pharmacol. Sci.* **2010**. 2010, 16.

6. Goia D.V.; Matijević, E. *New Journ. Chem*. **1998**. 11, 1203-1208.

7. Taleb, A.; Petit, C.; Pileni, M.P. *Chem. Mater*. **1997**. 9, 950-959.

8. Esumi, K.; Tano, T.; Torigoe, K.; Meguro, K. *Chem. Mater*. **1990**. 2, 564-567.

9. Henglein, A. *Langmuir*. **2001**. 17, 2329-2333.

10. Rodríguez-Sánchez, L.; Blanco M.C.; López-Quintela, M.A. *J. Physc. Chem. B*. **2000.** 104, 9683-9688.

11. Zhu, J.; Liu, S.; Palchik, O.; Koltypin, Y.; Gedanken, A. *Langmuir*. **2000**. 16, 6396-6399.

12. Pastoriza-Santos, I.; Liz-Marzán, L.M. *Langmuir*.

DOI: http://dx.doi.org/10.32571/ijct.1194356 **E-ISSN: 2602-277X**

2002. 18, 2888-2895.

13. Kröger, N.; Deutzmann, R.; Sumper, M. *Sci*. **1999**. 286, 1129-1132.

14. Ahmad, A.; Mukherjee, P.; Senapati, S.; Mandal, D.; Khan, M.I.; Kumar, R.; Sastry, M. *Coll. Surf. B: Biointer*. **2003**. 28, 313-318.

15. Shahverdi, A.R.; Minaeian, S.; Shahverdi, H.R.; Jamalifar, H.; Nohi, A.A. *Proc. Biochem*. **2007**. 42, 919-923.

16. Siddiqi, K.S.; Rashid, M.; Rahman, A.; Husen, A.; Rehman, S. *Biomat. Res.* **2018**. 22, 1-9.

17. Nath, D.; Banerjee, P. *Enviro. Toxicol. Pharm*. **2013**. 36, 997-1014.

18. Ovais, M.; Khalil, A.T.; Islam, N.U.; Ahmad, I.; Ayaz, M.; Saravanan, M.; Shinwari, Z.K.; Mukherjee, S. *Appl. Micr. Biotech*. **2018**. 102, 6799-6814.

19. Gardea-Torresdey, J.L. Gomez, E.; Jose, R.; Peralta-Videa, J.R.; Parsons, J.G.; Horacio, T.H.; Jose-Yacaman, M. *Langmuir*. **2003**. 19, 1357-1361.

20. Krishnaraj, C.; Ramachandran, R.; Mohan, K.; Kalaichelvan, P.T. *Spectro.Acta Part A: Mol. Biomol. Spectro*. **2012**. 93, 95-99.

21. Karthik, R.; Govindasamy, M.; Shen-Ming, C.S.; Cheng, Y.; Muthukrishnan, P.; Padmavathy, S.; Elangovan, A. *Jour. Photochem. Photo. B: Bio*. **2017**. 170, 164-172.

22. Chahardoli, A.; Karimi, N.; Fattahi, A. *Advanc. Pow. Techn*. **2017**. 29, 202–210.

23. Al-Otibi, F.; Perveen, K.; Al-Saif, N.A.; Alharbi, R.I.; Bokhari, N.A.; Al-Otaibi, R.M.; Al-Mosa, M.A. *Saudi Journ. Biol. Sci*. **2021**. 28, 2229–2235.

24. Le, N.T.T.; Trinh, B.T.; Nguyen, D.H.; Tran, L.D.; Luu, C.H,; Hoang Thi, T.T. *Journ. Clus. Sci.* **2021**. 32, 601-611.

25. Fatimah, I.; Hidayata, H.; Nugrohob, B.H.; Huseinc, S. *South Afr. Journ. Chem. Engin.* **2020**. 34, 97–106.

26. Kumar, B.; Smita, K.; Cumbal, L.; Debut, A. *Saudi Journ. Biol. Sci.* **2017**. 24, 45-50.

27. Bharadwaj, K.K.; Rabha, B.; Pati, S.; Choudhury, B.K.; Sarkar, T.; Gogoi, S.K.; Kakati, N.; Baishya, D.; Abdul, K.Z.; Edinur, H.A. *Nanomater*. **2021**. 11, 1999.

28. Sathishkumar, M.; Sneha, K.; Won, S.W.; Cho, C.W.; Kim, S.; Yun, Y.S. *Coll. Surf. B: Bioint.* **2009**. 73, 332-338.

29. Shetty, P.; Supraja, N.; Garud, M.; Prasad, T.N.V.K.V. *Journ. Nanostruc. Chem*. **2014**. 4, 161-170.

30. Arya, K.; Kumari, R.M.; Gupta, N.; Kumar, A.; Chandra, R.; Nimesh, S. *Artific. Cell. Nanomedic. Biotechnol.* **2018**. 46, 985-993.

31. Bankar, A.; Joshi, B.; Kumar, A.R.; Zinjarde, S. *Coll. Surf. A: Physic. Engin. Asp.* **2010.** 368, 58-63.

32. Behravan, M.; Panahi, A.H.; Naghizadeh, A.; Ziaee, M.; Mahdavi, R.; Mirzapour, A. *Inter. Journ. Biol. Macromol*. **2019**. 124, 148-154.

33. Venkatadri, B.; Shanparvish, E.; Rameshkumar, M.R.; Arasu, M.V.; Al-Dhabi, N.A.; Ponnusamy, V.K.; Agastian, P. *Saudi Journ. Biol. Sci*. **2020**. 27, 2980-2986.

34. Satpathy, S.; Patra, A.; Ahirwar, B.; Delwar, H.M. *Artific. Cell. Nanomedic. Biotechnol.* **2018**. 46, 71-85.

35. Bar, H.; Bhui, D.Kr.; Sahoo, G.P.; Sarkar, P.; Pyne, S.; Misra, A. *Coll. Surf. A: Physic. Engin. Asp*. **2009**. 348, 212-216.

36. Vidhu V.K.; Aromal, S.A.; Philip, D. *Spectr. Acta Part A: Molec. Biomol. Spectr*. **2011**. 83, 392-397.

37. Ya, T.; Ren, Z. *J. Syst. Evol*. **1996**. 34(3), 254-264.

38. Günal, N. *Act Turc*. **2013**. 5(1), 1-22.

39. Tuttu, G.; Ursavaş, S.; Söyler, R. *Anatol. J. For. Res*. **2017**. 3(1), 60-66.

40. Evans, W.C. *Trease and evans pharmacognosy, 16th edition*.; WB Saunders, Edinburg, 2010.

41. Guerin, J.C.; Reveillere, H.P. Antifungal activity of plant extracts used in therapy. *I Study of 41 plant extracts against 9 fungi species*; Annales Pharmaceutiques Francaises, 1984; pp 553-559.

42. Fitsiou, I.; Tzakou, O.; Hancianu, M.; Poiata, A. *J. Ess. Oil Res*. **2007**. 19, 183-185.

43. Bisset, N.G.; Wichtl, M. *Herbal drugs and phytopharmaceuticals*, CRC Press, Boca Raton, London, New York, Washington, 2001.

44. Konvičková, Z.; Holišová, V.; Kolenčík, M.; Niide, T.; Kratošová, G.; Umetsu, M.; Seidlerová, J. *Coll. Poly. Sci*. **2018**. 296(4), 677-687.

45. Cochran, W.G.; Cox, G.M. *Experimental designs*, 2nd ed. New York: USA, 1992.

46. Türkkan, M. *J. Agr. Sci*. **2013**. 19, 178-187.

47. Thompson, D.P. *Mycol*. 1989. 81, 151-153.

48. Tripathi, P.; Dubey, N.K.; Banerji, R.; Chansouria, J.P.N. *W. J. Micr. Biotech*. **2004**. 20, 317-321.

49. Veerasamy, R.; Xin, T.Z.; Gunasagaran, S.; Xiang, T.F.W.; Yang, E.F.C.; Jeyakumar, N.; Dhanaraj, S.A. *J. Saudi Chem. Soc*. **2011**. 15, 113-120.

50. Vanaja, M.; Gnanajobitha, G.; Paulkumar, K.; Rajeshkumar, S.; Malarkodi, C.; Annadurai, G. *J. Nano. Chem.* **2013**. 3, 1-8.

51. Khalil, M.M.; Ismail, E.H.; El-Baghdady, K.Z.; Mohamed, D. *Arab. J. Chem.* **2014**. 7(6), 1131-1139.

DOI: http://dx.doi.org/10.32571/ijct.1194356 **E-ISSN: 2602-277X**

52. Reddy, L.V.A.; Wee, Y.J.; Yun, J.S.; Ryu, H.W. *Bio. Techn*. **2008**. 99, 2242-2249.

53. Mondal, P.; Purkait, M.K. *Separ. Sci.Techn*. **2017**. 52, 2338-2355.

54. Cai, Y.; Piao, X.; Gao, W.; Zhang, Z.; Nie, E.; Sun, Z. *RSC Advan*. **2017**. 7(54), 34041-34048.

55. Nikaeen, G.; Yousefinejad, S.; Rahmdel, S.; Samari, F.; Mahdavinia, S. *Sci. Rep*. **2020**. 10, 1-16.

56. Mulvaney, P.,. *Langmuir*. **1996**. 12, 788-800.

57. Njagi, E.C.; Huang, H.; Stafford, L.; Genuino, H.; Galindo, H.M.; Collins, J.B.; Hoag, G.E.; Suib, S.L. Langmuir. **2011**. 27, 264-271.

58. Alahmad, A.; Al-Zereini, W.A.; Hijazin, T.J.; Al-Madanat, O.Y.; Alghoraibi, I.; Al-Qaralleh, O.; Al-Qaraleh, S.; Feldhoff, A.; Walter, J.G.; Scheper, T. *Pharm*. **2022**. 14(5), 1104.

59. Vijayaraghavan, K.; Nalini, S.P.K.; Prakash. N.U.; Madhankumar, D. *Mat. Lett*. **2012**. 75, 33–35.

60. Magudapathy, P.; Gangopadhyay, P.; Panigrahi, B.K.; Nair, K.G.M.; Dhara, S. *Physc. B: Conden. Matt*. **2001**. 299, 142-146.

61. Al-Zahrani, S.S.; Al-Garni, S.M. *J. Bio. Nanobiotech*. **2019**. 10, 11-25.

62. Ali, M.; Kim, B.; Belfield, K.D.; Norman, D.; Brennan, M.; Ali, G.S. *Phytopathol*. **2015**. 105, 1183-1190.

63. Buzea, C.; Pacheco, I.I.; Robbie, K. *Biointerph*.. **2007**. 2, 17-64.